Current Research (2015) Newfoundland and Labrador Department of Natural Resources Geological Survey, Report 15-1, pages 43-61

THE GEOLOGY AND GENESIS OF THE KEATING HILL Fe–Ti–V PROSPECT, MAIN GUT INTRUSION (NTS MAP AREAS 12A/05 AND 12B/08), WESTERN NEWFOUNDLAND

J.G. Hinchey
Mineral Deposits Section

ABSTRACT

The Keating Hill Fe–Ti–V prospect is hosted within cumulate gabbroic to gabbronoritic rocks of the Silurian Main Gut mafic intrusion of the Puddle Pond complex, in western Newfoundland. Although oxide mineralization was originally discovered in the area in the 1930s, the first significant exploration activity was not conducted until 2009.

The prospect is host to two styles of oxide mineralization, which have differing oxide textural relationships. The earlier style occurs as intercumulus oxides formed by fractional crystallization processes from a magma also producing hydrous hornblende oikocrystic gabbronorite. Oxide minerals in this style of mineralization locally accumulated by gravitational settling of intercumulus liquid to form stratigraphically defined layers of semi-massive oxide. These layers display sharp basal contacts and gradational upper contacts. Oxide mineralization is composed of intergrown magnetite and ilmenite. The magnetite is devoid of spinel exsolution, but ilmenite contains titanomagnetite exsolution. This style of mineralization displays fractionated REE patterns with increased LREE on chondrite-normalized plots, and displays negative HFSE (Th, Nb, Zr, Hf) anomalies on primitive mantle-normalized trace-element plots.

The later style of oxide mineralization is composed of semi-massive to massive oxides that appear to have invaded partially solidified host rocks. The mineralization is interpreted to have formed via *liquid immiscibility from the same parental magma. Such an origin is at odds with more conventional models for oxide accumulation in which gravity is the driving force in the formation of massive mineralization. Features supporting the invasive style of mineralization include: 1) sharp upper and lower contacts on the semi-massive to massive style of mineralization, 2) disequilibrium textures between oxide and silicate minerals, observed as reaction rims and thermal erosive contacts, and 3) the local presence of gabbroic inclusions occurring in the semi-massive to massive oxide mineralization. As with the intercumulus mineralization, this style of mineralization displays fractionated REE patterns with increased LREE on chondrite-normalized plots, but, in contrast to the intercumulus mineralization, it displays positive HFSE (Th, Nb, Zr, Hf) anomalies on primitive mantle-normalized trace-element plots.*

Several Silurian mafic intrusions throughout central and western Newfoundland contain minor occurrences of magmatic sulphide mineralization, but the Keating Hill body represents a newly recognized style of magmatic oxide mineralization, for which similar potential may exist in other Silurian mafic intrusions in the region.

INTRODUCTION

PROJECT DESCRIPTION

The Keating Hill Fe–Ti–V prospect is located in the Notre Dame Subzone of the Dunnage Zone, southwestern Newfoundland, and straddles the Puddle Pond (NTS map area 12A/05) and Main Gut (NTS map area 12B/08) map areas (Figure 1). The prospect is hosted by mafic intrusive rocks, denoted as Unit Spc on Figure 1, of the *ca.* 431 Ma Puddle Pond complex (van Staal *et al.*, 2005; Pehrsson *et al*., 2013), and contains disseminated to semi-massive and massive magmatic oxide mineralization. The style of mineralization comprises stratiform zones of possible intercumulus origin and massive material that appears invasive.

This report presents observations and interpretations derived from field and petrographic observations and lithogeochemical data. Information on mineral textures, and oxide mineral chemistry was obtained *via* scanning electron microscope–mineral liberation analysis (SEM–MLA) and electron microprobe methods.

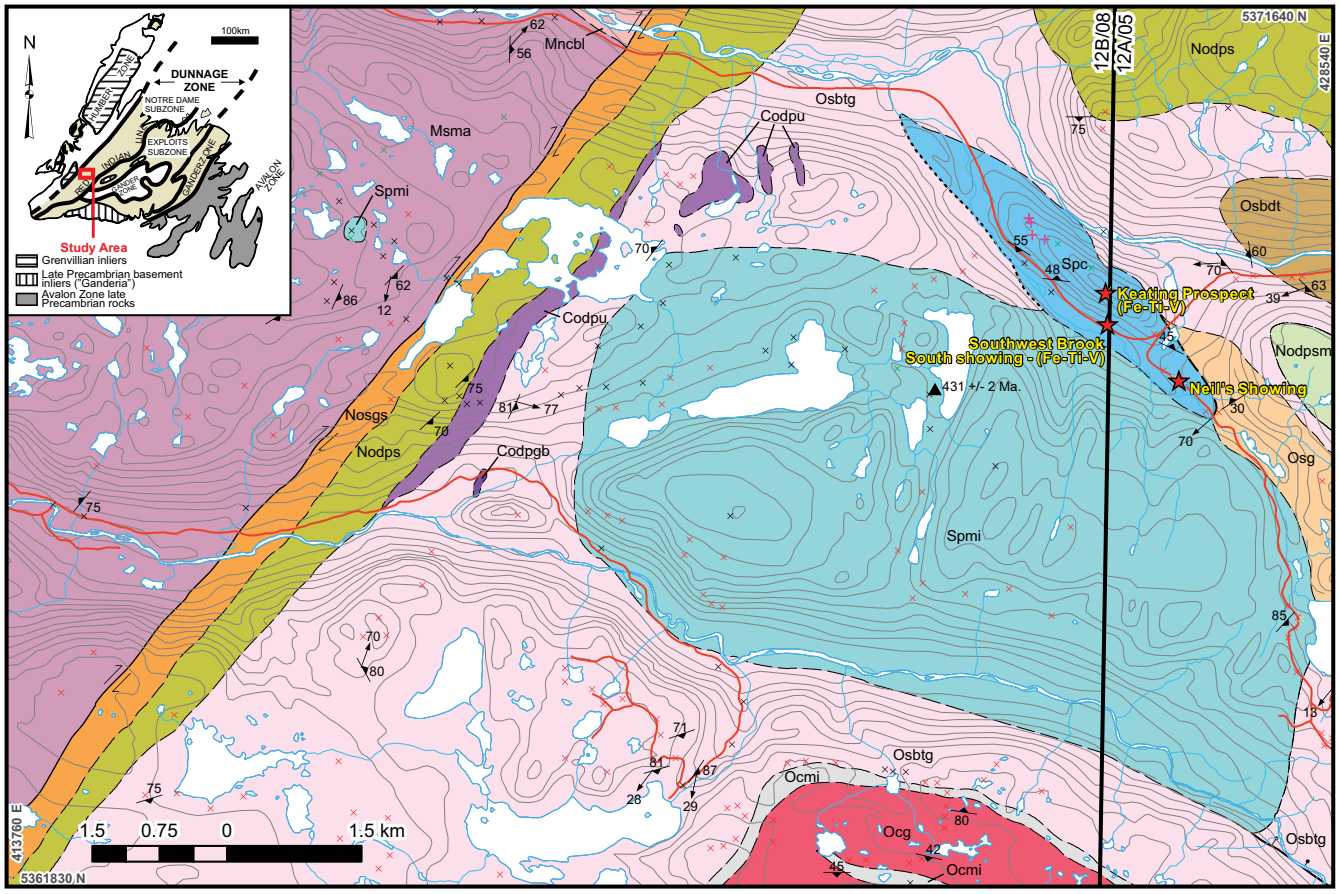

Figure 1. *Regional geological map of the area around the Keating Hill Fe–Ti–V prospect (modified after van Staal* et al.*, 2005 and Pehrsson* et al.*, 2013). Only the mineral occurrences noted in the text are displayed on the map. Inset regional map of Newfoundland shows the project location. Legend modified from van Staal* et al. *(2005) and Pehrsson* et al. *(2013). Legend for Figure 1 on opposite page.*

PREVIOUS WORK AND EXPLORATION HISTORY

Regional Mapping Programs

Early regional mapping in the area was conducted by Riley (1957) and Barnes *et al*. (1957) at a scale of 1 inch to 4 miles. The Keating Hill area was assigned as undivided granite and gneiss belonging to the Long Range igneous and metamorphic complex and no gabbroic rocks were identified. Carew (1979) completed a B.Sc. (Hons) thesis including field work, petrography and geochemical investigations, and reported a cumulate norite body approximately 2.5 km long in the vicinity of the Keating Hill property. He described the norite as containing spectacular magnetite-rich layers, oriented north–south dipping steep westerly, and having individual layers up to 15 cm thick. He also recorded local examples of crossbedding in the magnetite layers, which he suggested were formed by magmatic convective currents. The layered norite was interpreted to be differentiated from a more massive gabbroic intrusive body located immediately to the south, which was later dated at 431 ± 2 Ma (Dunning *et al*., 1990).

The area of the southern Long Range Mountains was the focus of a multi-year mapping program as part of the Canada–Newfoundland Mineral Development Agreement from 1984-1989. Mapping completed by the Geological Survey of Canada is summarized in a 1:100 000 scale map and accompanying notes (Currie and van Berkel, 1992 a, b). These authors assigned the host rocks of the Keating Hill prospect to the Silurian Main Gut intrusive complex, intruding into the Central Gneiss subzone of the southern Long Range Mountains (Currie and van Berkel, 1992b). As with Carew (1979), these authors describe the rocks as being composed of massive, relatively unaltered gabbroic rocks having igneous layering defined by magnetite.

The area was recently remapped by the Geological Survey of Canada. The Puddle Pond map area (NTS 12A/05) was mapped by van Staal *et al*. (2005), and the Main Gut

LEGEND (Figure 1, opposite page**)**

Silurian

Puddle Pond Complex (ca. 431 Ma)

Spmi — Foliated to unfoliated, dark grey to green, mainly medium- to coarse-grained, partly amphibolitized equigranular to plagioclase-phyric hornblende diorite, gabbro, or diabase. Gabbro locally contains layers of pyroxenite and pegmatitic pods. Mafic rocks commonly have mixed arc to non-arc-like compositions

Spc — Foliated to unfoliated, mainly layered cumulate sequence of anorthosite, troctolite, olivine norite, norite, gabbronorite, olivine gabbro, and gabbro, with minor pyroxenite. Minor alteration to epidote, hornblende and/or actinolite and chlorite

Ordovician

Southwest Brook Complex (ca. 461 Ma)

Osbtg — Generally well-foliated, white, medium- to coarse-grained, mainly biotite- and/or hornblende-bearing, tonalite and/or granodiorite. Locally includes crosscutting gabbro or diorite of the Puddle Pond complex (Unit Spmi)

Osbdt — Generally well-foliated, medium- to coarse-grained, biotite and hornblende-bearing quartz diorite and/or tonalite

Osg — Foliated to unfoliated biotite granodiorite and/or granite, locally with K-feldspar megacrysts

Neoproterozoic to Middle Ordovician

Cormacks Lake Complex (> 455 Ma)

Ocg — Mainly well-banded granodiorite to tonalite orthogneiss (ca. 483 Ma)

Ocmi — Metagabbro, orthopyroxene- and/or clinopyroxene-bearing

Dennis Pond Complex (> 488 Ma)

Codpgb — Mainly gabbro. Includes minor troctolite and trondhjemite

Codpu — Mainly layered ultramafic rock. Includes dunite, harzburgite, lherzolite, wehrlite websterite, pyroxenite, and minor gabbro and trondhjemite. Locally contains chromite-rich layers

Nodpsm — Characteristically unlayered and chaotic, strongly metamorphosed and migmatitic melange, consisting of abundant large blocks and cobbles of mafic rocks in a pelitic to semipelitic matrix

Nodps — Mainly chlorite and muscovite bearing schistose mixture of granitoid rocks and metasediments, with local tectonic inclusions of other Dennis Pond complex units

Nosgs — Tectonic zone consisting of greenschist mylonite and cataclasite, strongly deformed paragneiss, orthogneiss, granite and anorthosite

Neoproterozoic and older

Steel Mountain Complex

Msma — Massive to strongly foliated pegmatitic anorthosite, gabbroic anorthosite and anorthosite gneiss, cumulate textures along the margin.

Undifferatiated Corner Brook Lake Complex (ca. 1510 Ma)

Mncbl — Quartzofeldspathic gneiss and migmatite, with interbanded amphibolite, minor quartzite, marble, and quartz-feldspar-mica paragneiss and orthopyroxene-bearing gneisses

Fault, normal, approximate

Fault, strike-slip, dextral, assumed

Fault, approximate

Fault, assumed

Contact, approximate

Foliation: main and/or composite

Lineation

Diamond drill hole

Mineral occurrence

Outcrop - compiled historic

Outcrop - GSC TGI3

Outcrop - this study

Forestry roads

Geochronology site

map area was mapped by Pehrsson *et al*. (2013). They interpret the host to the Keating Hill prospect as part of the Puddle Pond complex (Figure 1, Unit Spc; *ca*. 431 Ma), composed of a foliated to unfoliated, layered mafic cumulate sequence intruding Ordovician tonalite and granodiorite.

Exploration History

The earliest description of the Keating Hill prospect is by Thomson (1941), who was investigating a magnetite occurrence found by Mr. J. Keating in the early 1930s. Thomson noted that all rocks in the area were igneous and that magnetite occurred in many places as seams and individual crystals. He noted a black rock, composed of magnetite, amphibole, pyroxene and minor plagioclase, which he suggested, could have economic significance. He also recorded a magnetite-rich rock having sharp contacts with the surrounding gabbro, suggesting that the magnetite-rich rocks represented 'segregations' in the gabbro.

Prospecting led by L. Muise from 2007 through to 2009 returned vanadium grades ranging up to 0.358% V_2O_5 (as with all vanadium grades quoted herein V_2O_5 was calculated as V_2O_5 (%) = 1.78 * 10^{-4} * V (ppm)) associated with magnetite-rich gabbroic rocks (French and Mugford, 2010). The map staked licenses eventually became part of exploration licenses held by Triple Nine Resources, who have completed extensive prospecting, geochemical, and geophysical work, and approximately 4000 m of diamond drilling on the property (French and Mugford, 2010, *http://tripleninesources.com*). This work identified a potentially significant Fe–Ti–V mineralized zone on the property. Most of the work and interpretations presented in this report are derived from detailed logging of diamond-drill core from the area. Core examined for this report is presently stored in the Department of Natural Resources core library in Buchans.

REGIONAL OVERVIEW

The rocks in the study area formed along the peri-Laurentian margin of the ancient Iapetus Ocean (Williams, 1995), as part of the continental Notre Dame arc (Whalen *et al*., 2006), and associated remnant ophiolitic rocks. Ordovician to Silurian plutonic rocks are abundant and represent varied environments (*e.g*., Currie and van Berkel, 1989; Lissenberg *et al*., 2006; Whalen *et al*., 2006; van Staal *et al*., 2007). Plutonic rocks have been linked to west-directed subduction beneath the Laurentian margin (Lissenberg *et al*., 2005; van Staal *et al*., 2007), which was responsible for several magmatic episodes. These include voluminous tonalite plutonism (*ca*. 466–459 Ma), as well as ophiolite accretion to the Laurentian margin (*e.g.*, Lissenberg *et al*., 2006; Whalen *et al*., 2006). Closure of the main tract of the Iapetus Ocean juxtaposed the peri-Laurentian rocks against those of peri-Gondwanan affinity (*e.g.*, Victoria arc, Zagorevski *et al*., 2007). Continued accretion of outboard terrains (*e.g.*, Ganderia, Figure 1, inset) *via* west-directed subduction coincided with the waning stages of the Notre Dame arc. The plutonic history eventually culminated with widespread Silurian magmatism that includes the host rocks of the Keating Hill prospect (Puddle Pond complex).

KEATING HILL PROPERTY

LOCAL GEOLOGY AND MINERALIZATION

The Keating Hill prospect is hosted by the 431 Ma Puddle Pond complex (van Staal *et al*., 2005; Pehrsson *et al*., 2013), which outcrops over a geographically large area (units Spmi and Spc on Figure 1; previously grouped and referred to as the Main Gut intrusion (Carew, 1979) or the Main Gut complex (van Berkel, 1987)). The oxide mineralization at the Keating Hill prospect is hosted in Unit Spc (Figure 1). Unit Spc outcrops as a northwest-trending, lens-shaped layered intrusion exposed over approximately 5 x 1 km (van Staal *et al*., 2005; Pehrsson *et al*., 2013), within which cumulate layers strike northwest and dip approximately 55–60° west. The unit is described as *"a foliated to unfoliated, mainly layered cumulate sequence of anorthosite, troctolite, olivine norite, norite, gabbronorite, olivine gabbro, and gabbro, with minor pyroxenite"* (van Staal *et al*., 2005; Pehrsson *et al*., 2013). Rock types observed in this study generally lack olivine, however, this general description encompasses rocks farther to the east that are more mafic (*cf.,* Hinchey, 2013). Outcrop observations and examination of five diamond-drill holes indicate a layered sequence of leucogabbro, leucogabbronorite, gabbro, gabbronorite, and hornblende oikocrystic gabbronorite (Plate 1A). Olivine-bearing rock types were only locally observed near the bottom of some diamond-drill holes (*e.g.,* FCP-04-10) and in the vicinity of Neil's prospect, which occurs at a lower elevation relative to the main Keating Hill prospect (Figure 1). Although all rock types commonly contain some oxide minerals, the gabbronorite and hornblende oikocrystic gabbronorite host the most significant oxide mineralization. Magnetite and ilmenite occur either as intercumulus disseminations, or as semi-massive to massive invasive mineralization (Plate 1B, C).

Contacts between rock types in drillcore are generally sharp and are defined by proportions of oxide minerals or silicate mineral phases, or grain-size variations. Aside from local chilling at contacts between coarse-grained gabbro and other rock types, chilled contacts are typically absent, suggesting largely synchronous emplacement of intrusions. Many contacts in diamond-drill core are defined by faults. Pegmatitic segregations have subophitic to ophitic textures,

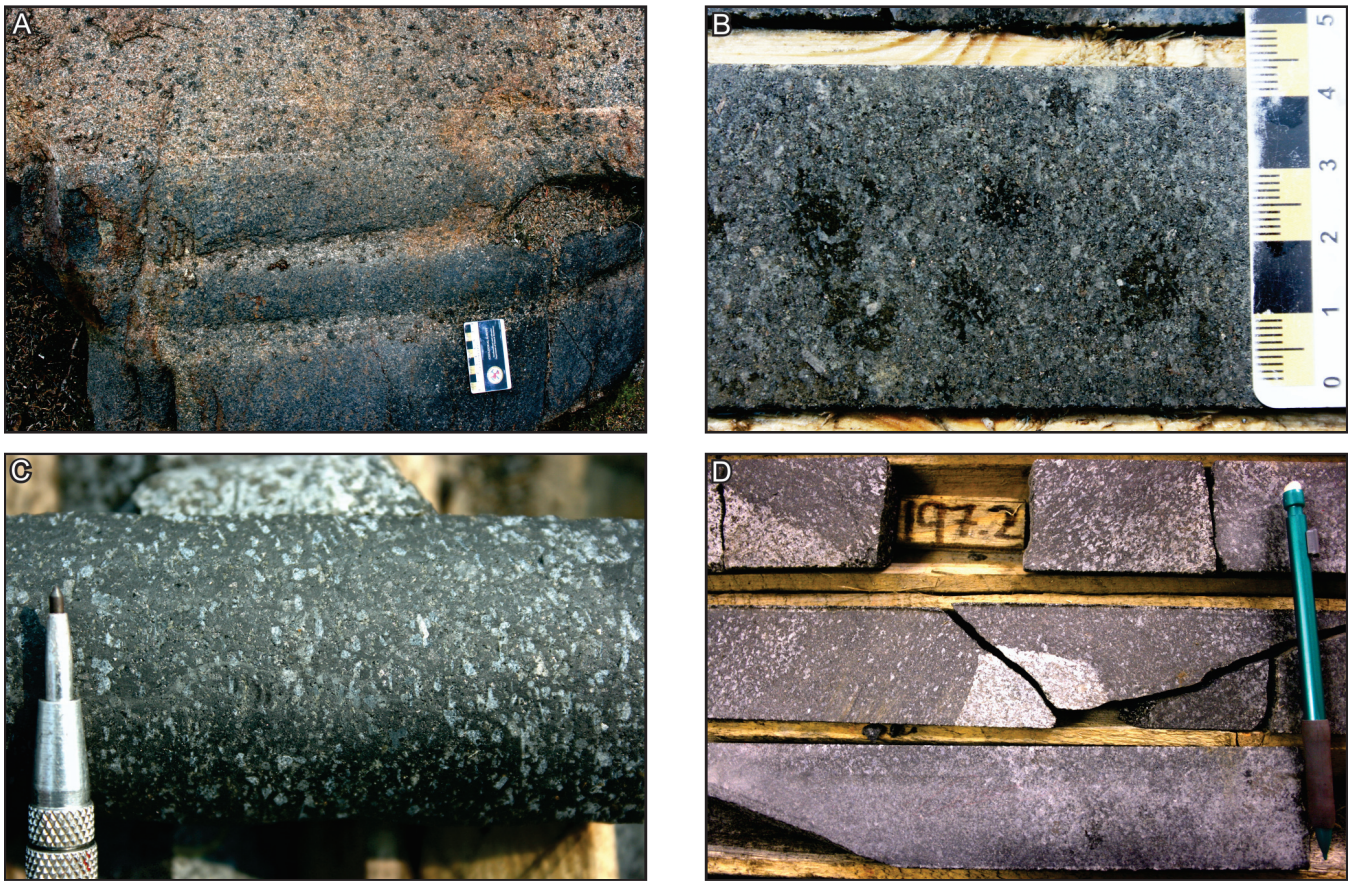

Plate 1. A) *Example of massive oxide horizons in a hornblende oikocrystic gabbronorite – Keating Hill exploration trench;* B) *Example of intercumulus oxide mineralization in the hornblende oikocrystic gabbronorite (FCP-03-10 @ 45 m);* C) *Semi-massive oxide mineralization interpreted to have invaded a crystal mush of the parental hornblende oikocrystic gabbronorite (FCP-03-10 @ 64.5 m); and* D) *Example of an inclusion of gabbroic material in the invasive style of semi-massive to massive oxide mineralization (FCP-04-10 @ 198.5 m).*

and contain plagioclase crystals up to 4 cm long. Most rock types contain primary hornblende, biotite, or phlogopite, suggesting crystallization from hydrous magmas. Rocks are generally fresh and unfoliated.

Oxide mineralization is mostly hosted by the hornblende oikocrystic gabbronorite, with some semi-massive oxide mineralization hosted in gabbro. Oxides are composed of magnetite and ilmenite, and are commonly associated with minor magmatic sulphide blebs composed of pyrrhotite and pyrite, and lesser chalcopyrite and pentlandite. Visual estimates range from approximately 5% oxides for weakly disseminated and intercumulus mineralization up to greater than 60-70% oxides for semi-massive to massive mineralization.

Textural relationships between silicates and oxides vary. Locally, there is evidence for accumulation of oxides *via* gravity-driven, dense intercumulus liquid settling in a cumulate pile, resulting in an increase in the proportion of oxides near the base of a mineralized interval, culminating in semi-massive oxide layers. These basal oxide layers have sharp lower contacts and gradational upper contacts. Other examples of semi-massive to massive oxides display sharp upper and lower contacts and appear to represent an oxide-rich liquid that has invaded an unconsolidated silicate mush. This interpretation is supported by the presence of plagioclase crystals (locally aligned) entrained in semi-massive oxides. The latter style of mineralization also locally includes discrete inclusions of gabbroic material containing minor oxides, which have sharp, well-defined contacts. Such features also suggest an invasive style of mineralization (Plate 1D).

Concentrations of $Fe_2O_3^T$, TiO_2 and V_2O_5 are highest in semi-massive mineralization hosted by hornblende oikocrystic gabbronorite. Examples of grades of mineralization from the property include diamond-drill hole FCP-01-10, which intersected 21.82% $Fe_2O_3^T$, 5.08% TiO_2, and 0.116% V_2O_5 over 217 m. Within this hole, which is miner-

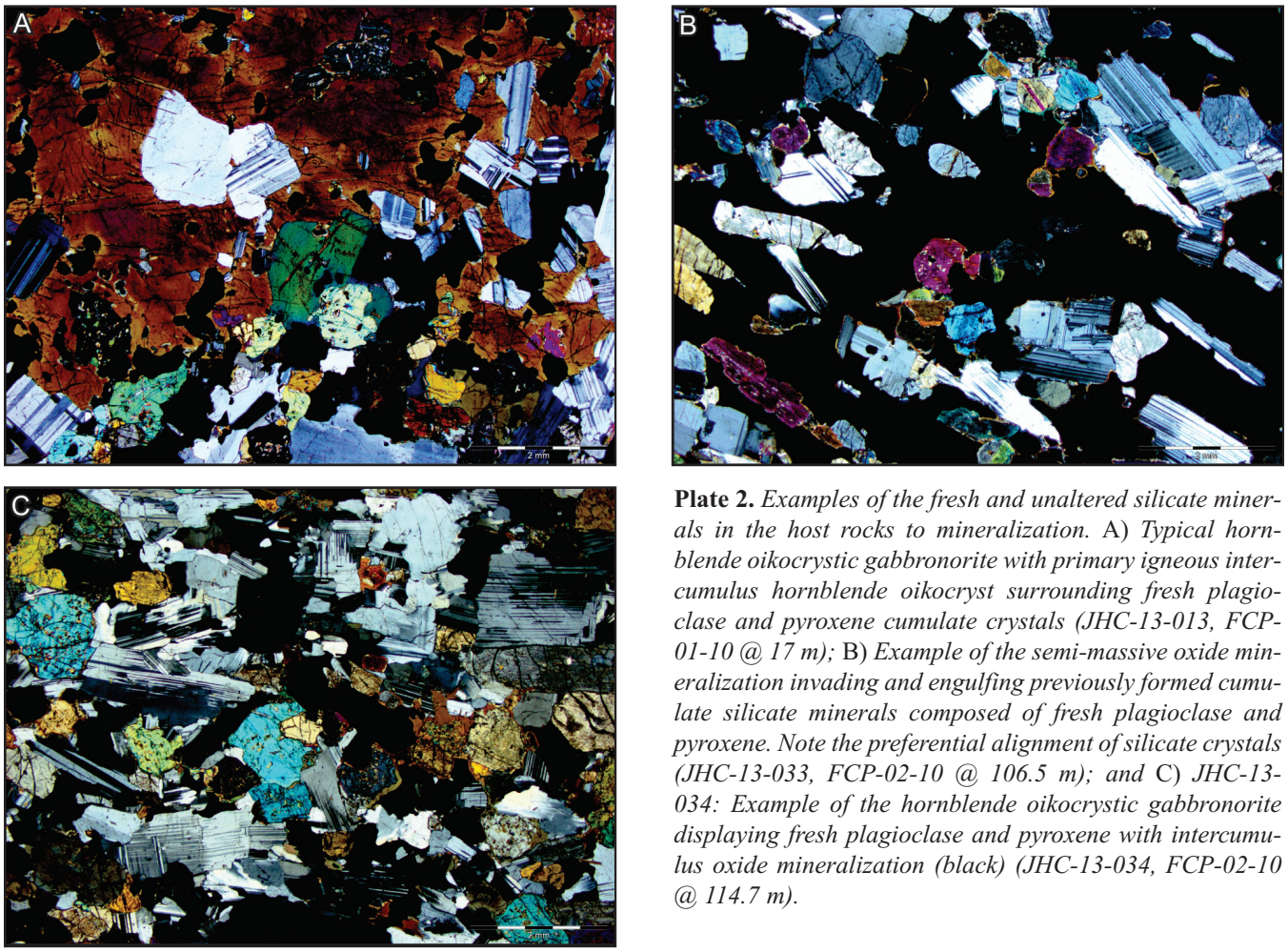

Plate 2. *Examples of the fresh and unaltered silicate minerals in the host rocks to mineralization.* A) *Typical hornblende oikocrystic gabbronorite with primary igneous intercumulus hornblende oikocryst surrounding fresh plagioclase and pyroxene cumulate crystals (JHC-13-013, FCP-01-10 @ 17 m);* B) *Example of the semi-massive oxide mineralization invading and engulfing previously formed cumulate silicate minerals composed of fresh plagioclase and pyroxene. Note the preferential alignment of silicate crystals (JHC-13-033, FCP-02-10 @ 106.5 m); and* C) *JHC-13-034: Example of the hornblende oikocrystic gabbronorite displaying fresh plagioclase and pyroxene with intercumulus oxide mineralization (black) (JHC-13-034, FCP-02-10 @ 114.7 m).*

alized throughout, there is a higher grade section of 28.9 m grading 42.74% $Fe_2O_3^T$, 9.62% TiO_2, and 0.227% V_2O_5 (French and Mugford, 2010).

PETROLOGY

The primary igneous minerals are well preserved (Plate 2A–C). The mineral assemblage is dominated by medium-grained, sub- to euhedral plagioclase, orthopyroxene, clinopyroxene, and hornblende. Brown mica, magnetite, ilmenite, and minor phases such as sulphide and apatite are also present. Olivine forms anhedral crystals in some of the mineralized rocks, but appears to be limited to deeper parts of the intrusion. The main host rock to the oxide mineralization contains large (cm-scale) intercumulus hornblende oikocrysts, containing smaller cumulus plagioclase and pyroxene crystals, as well as brown mica (Plate 2A). The oikocrysts are less obvious in the invasive style of semi-massive to massive mineralization, but this may reflect difficulty of observation due to the increased percentage of oxide minerals, or the absorption of silicate phases by the

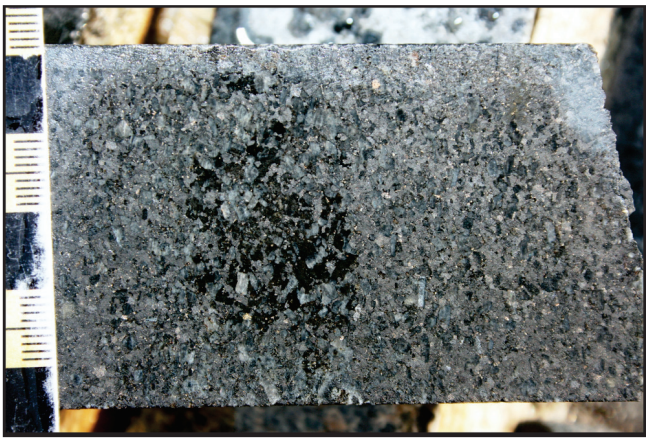

Plate 3. *Example of the semi-massive invasive style of oxide mineralization with the hornblende oikocrysts in the host preserved (FCP-03-10 @ 45 m).*

invasive oxide liquid (*see* below). In some examples, hornblende oikocrysts are still plainly visible in semi-massive mineralization (Plate 3), confirming the common host. Inter-

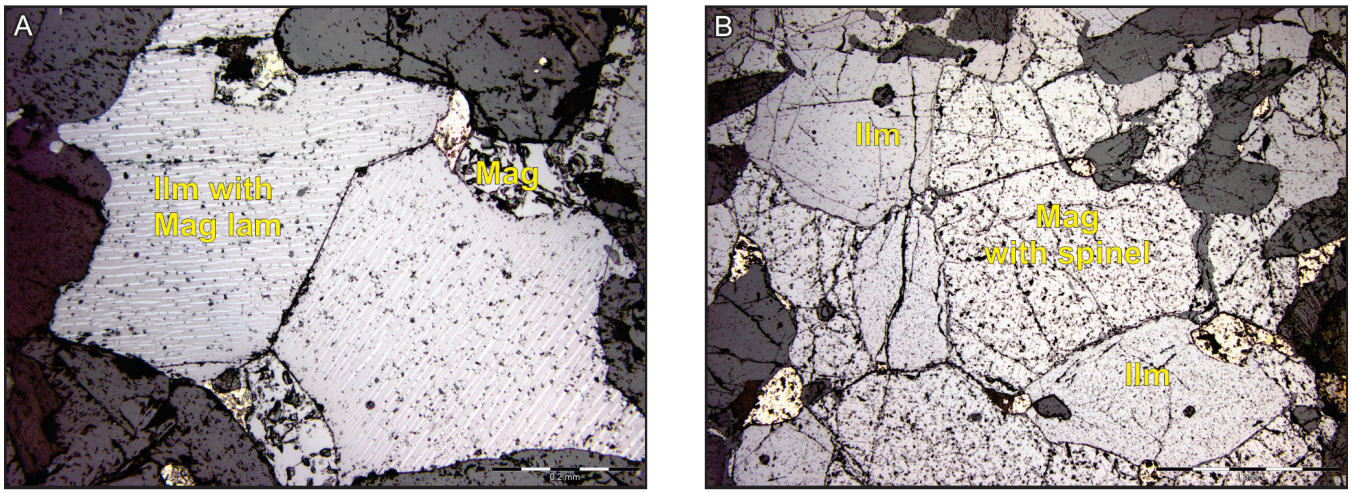

Plate 4. A) *Intercumulus oxide mineralization occurring in the hornblende oikocrystic gabbronorite. Oxides are composed of magnetite, which is devoid of any exsolution phases, and ilmenite, which contains exsolution lamellae of titanomagnetite (JHC-13-034, FCP-03-10 @114.7 m); and* B) *Example of semi-massive oxide mineralization enclosing silicate minerals. Oxides are composed of ilmenite, which is devoid of any exsolution phases, and magnetite with spinel exsolutions (JHC-13-033, FCP-03-10 @ 106.5 m). Note the presence of sulphide blebs in both styles of mineralization.*

cumulus minerals, in addition to the hornblende oikocrysts, are dominated by apatite and zircon. The mineralized rocks contain abundant variably textured magnetite and ilmenite, and minor magmatic sulphide.

The coarse-grained gabbroic rocks commonly display an ophitic to subophitic texture in which pyroxene surrounds plagioclase, whereas the main host to the oxide mineralization commonly displays a poikilitic texture having plagioclase and pyroxene as cumulus minerals within hornblende oikocrysts.

Oxide Mineralization

Oxide mineralization, occurring as intergrown magnetite and ilmenite, occurs in a variety of habits. Mineralization is predominantly hosted within the hornblende oikocrystic gabbronorite, with only minor examples of significant concentrations of oxides occurring in gabbro. Oxides occur as intercumulus space fillings between cumulate silicate minerals in disseminated styles of mineralization (Plates 2C and 4A). This style of mineralization locally becomes semi-massive due to intercumulate liquid settling. The disseminated oxides are commonly accompanied by apatite and zircon (*see* below). In semi-massive to massive mineralization, oxide minerals completely enclose silicate minerals, displaying abrupt upper and lower contacts with the host hornblende oikocrystic gabbronorite (Plates 2B and 4B). Further, the textures suggest that this mineralization is invasive. This suggests that Fe–Ti–V oxides formed both through direct precipitation from the parental magma, and also formed a Fe–Ti–V oxide liquid that separated immiscibly from the host magma. In the latter case, reaction rims composed of variable amounts of hornblende, mica, and/or olivine are ubiquitous between the oxide minerals and the silicate phases dominated by plagioclase and pyroxene (Plate 5A, B). In addition, the latter style of mineralization commonly displays plagioclase crystals that have been thermally eroded, and embayed/resorbed, by the Fe–Ti–V oxide liquid. These features appear as scalloped or embayed contacts where plagioclase twins and grain boundaries are truncated, and, as such, the observed reaction rims could not represent late-stage interstitial minerals (Plate 6A, B). Such reaction rims also occur in the former style of mineralization, but are not ubiquitous. These textures and reaction rims are indicative of hydrous magmas, and suggest that a dense iron-rich oxide melt or liquid was injected into a silicate crystal mush at a relatively late stage of crystallization. This style of oxide mineralization contrasts with the stratiform oxide-rich disseminated layers within the layered intrusion. The stratiform mineralization appears to have a primary magmatic origin where oxides crystallized from a relatively late-stage interstitial oxide liquid. The local presence of rounded sulphide droplets within oxide minerals in both styles of mineralization also points to a dominant magmatic control on the mineralizing processes (*e.g.*, Plate 4A, B).

Textural relationships amongst oxide minerals show two main types. In the first type, oxide mineralization, in which early formed ilmenite crystals contain fine lamellae of titanomagnetite (*see* below), is intergrown with magnetite crystals devoid of internal intergrowths (Plate 4A). In the second, relatively coarse-grained blebby oxide intergrowths contain early crystallized ilmenite (free of any internal intergrowths) and occur with magnetite containing spinel exsolution (Plate 4B). These textural subtypes correspond to the

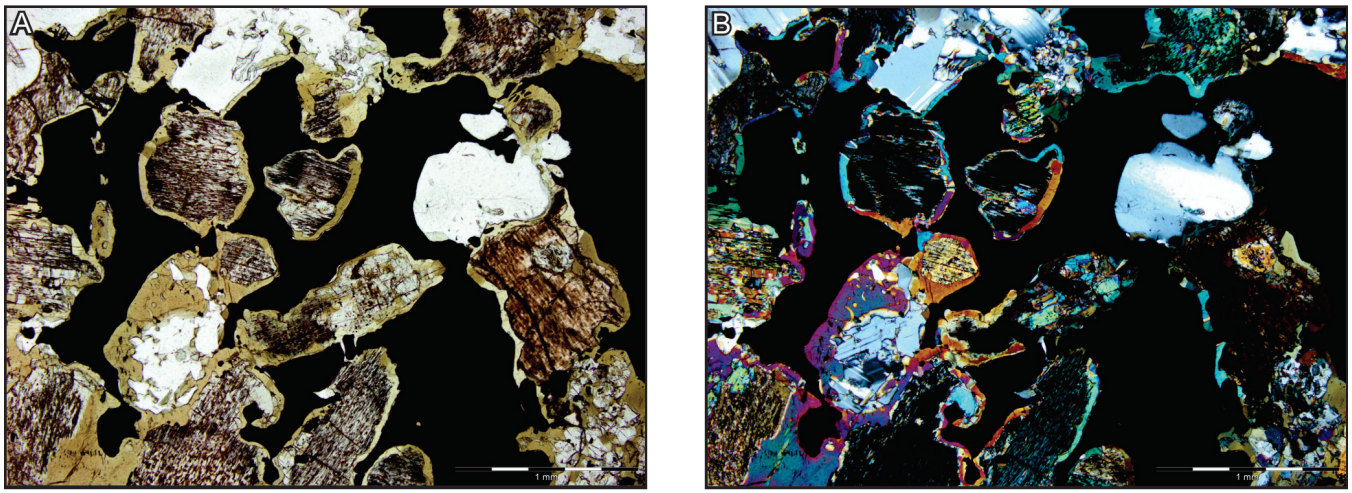

Plate 5. A) *Example of the semi-massive invasive style of oxide mineralization illustrating the ubiquitous reactions rims, in this case dominated by hornblende, occurring at the oxide (black) and silicate interface and indicative of disequilibrium conditions; and* B) *as in A with cross-polarized light (JHC-13-025, FCP-01-10 @ 194.5 m).*

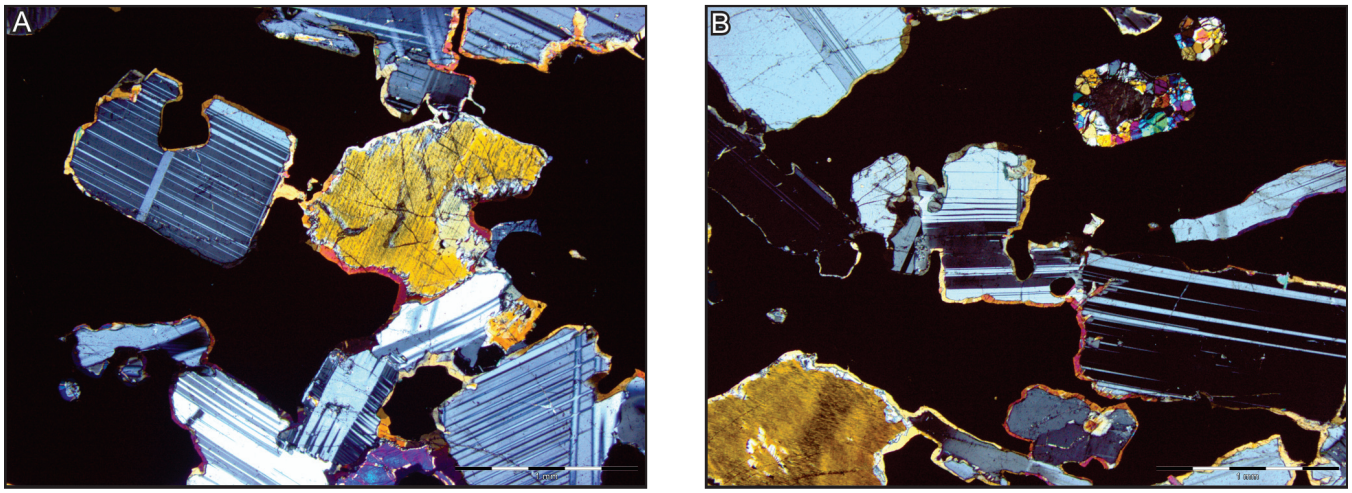

Plate 6. *Example of thermal erosion of silicate grain boundaries by the invasive semi-massive to massive oxide melt.* A) *Thermal erosion of silicate minerals (plagioclase and pyroxene) illustrated by the scalloped and embayed grain margin of plagioclase cutting through plagioclase twinning, as well as the ubiquitous rims of hornblende surrounding the silicates; and* B) *similar to A with hornblende and olivine forming the reaction rims on the silicates. Both plates from JHC-14-009 from FCP-03-10 @63.6 m.*

disseminated intercumulus and to the invasive semi-massive to massive mineralization, respectively. Initial petrographic observation tentatively identified the lamellae within the ilmenite as being composed of magnetite based on the observation that the lamellae were isotropic whereas the ilmenite is anisotropic, and this has been confirmed through subsequent SEM–MLA and electron microprobe work (*see* below).

Scanning Electron Microscopy–Mineral Liberation Analysis (SEM–MLA) Techniques

One thin section of the disseminated intercumulus style of mineralization was examined using SEM–MLA techniques at Memorial University. Results suggested that the lamellae in the ilmenite are composed of Ti-rich magnetite, and, as observed petrographically, the lamellae decrease in abundance as the contact with pure magnetite or sulphide is approached (Plate 7A, B). In addition, the SEM–MLA techniques also identified abundant apatite and zircon in association with the intercumulus oxide mineralization (Plate 7A, B), and confirmed petrographic observations of sulphides. Although the iron and titanium contents of minerals could be confirmed, it was not possible to define vanadium distribution using the SEM–MLA techniques. As such, additional mineral composition evaluations were conducted *via* electron microprobe methods.

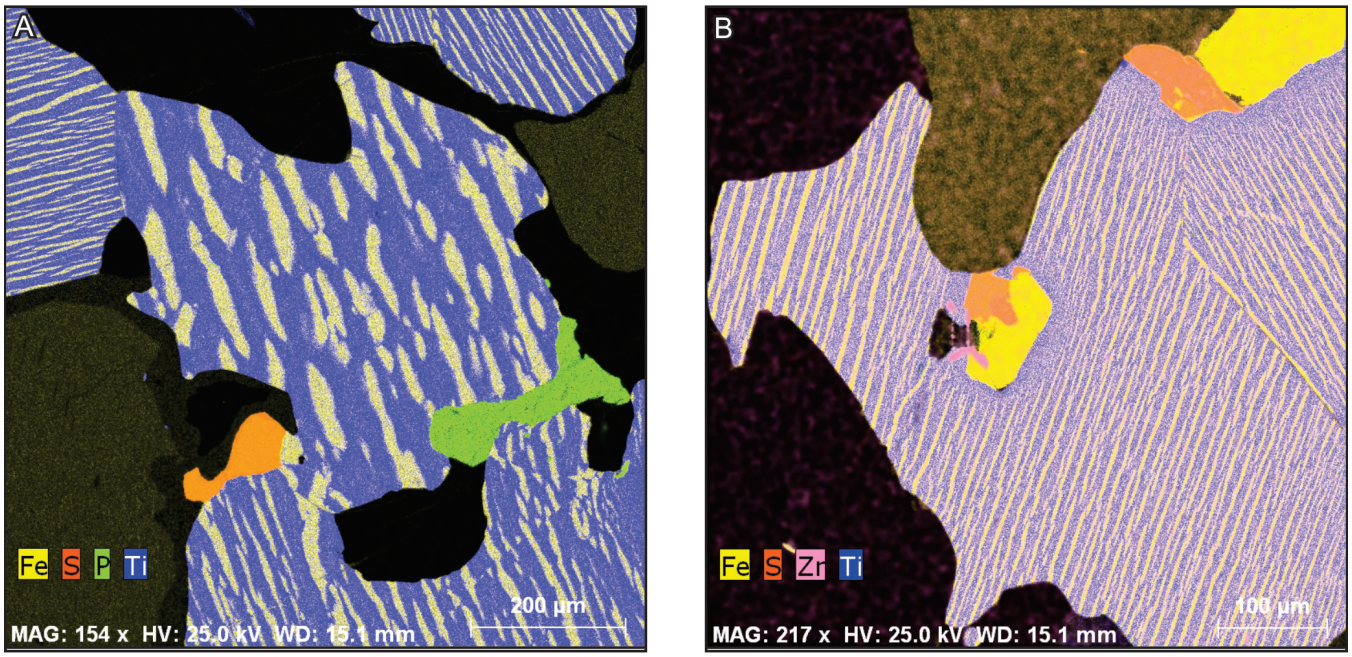

Plate 7. *SEM–MLA images from an example of the intercumulus style of mineralization (JHC-13-034, FCP-03-10 @ 114.7 m).* A) *Image illustrating the titanomagnetite lamellae (pale yellow) in ilmenite (blue). Note also apatite (green) and sulphide (orange); and* B) *Image illustrating the titanomagnetite lamella as well as zircon (pink) and sulphide. Note the decrease in lamellae concentration as the coarser grained magnetite (yellow) is approached.*

Electron Microprobe Analysis

Further investigations were conducted by wavelength-dispersive X-ray spectrometry methods using a Cameca microprobe at Carleton University, under the guidance of Mr. P. Jones. Two samples were analyzed; one from the disseminated intercumulate mineralization displaying the lamellae in the ilmenite (the same sample as used for SEM–MLA), and one from the semi-massive to massive style of mineralization that does not contain lamellae in ilmenite. This work was aimed at determining the composition of the lamellae within the ilmenite of the intercumulus mineralization, and also to document any contrasts in Fe, Ti, V, and other trace-element abundances between the two styles of mineralization. Analytical results are given in Table 1, with FeO and Fe_2O_3 calculated based on stoichiometric considerations following the methods of Droop (1987). The fact that the vanadium K-alpha X-ray line is partially overlapped by the titanium K-beta X-ray line required careful analysis to determine vanadium concentrations. Careful selection of background positions for the analysis of vanadium in the presence of high titanium essentially eliminated this problem, and analyzed synthetic standards containing high titanium ($MnTiO_3$ and TiO_2) gave essentially a value of zero for vanadium.

As suggested by petrographic work and SEM–MLA techniques, electron microprobe work confirmed that the lamellae in the ilmenite from the disseminated style of mineralization are magnetite, but also contain significant titanium (Table 1). When plotted on a TiO_2–FeO–Fe_2O_3 (with subordinate oxides included) ternary diagram, the titanomagnetite lamallae compositions fall on the solid-solution tie line between pure stoichiometrically calculated magnetite and ulvospinel; indicative of ionic substitution (Figure 2). In contrast, all ilmenite compositions plot toward the pure stoichiometrically calculated ilmenite composition of the tie line representing solid solution between ilmenite and hematite (Figure 2). This result is different from that determined by Actlabs (French and Mugford, 2010) who, based on SEM–MLA techniques, reported that the lamallae were composed of hemo-ilmenite.

There are also variations in the compositions of the magnetite and ilmenite from the two styles of mineralization (Table 1). As noted above, magnetite occurs in three different forms: 1) as coarse magnetite in the disseminated mineralization, 2) as fine lamellae within ilmenite in the disseminated mineralization, and 3) as coarse magnetite with spinel exsolutions in the semi-massive to massive style of mineralization.

The coarse-grained magnetite in both styles of mineralization has higher proportions of FeO^T compared to the magnetite lamellae in the disseminated mineralization, which contain significantly higher titanium (Table 1). The V_2O_5 concentrations are elevated in all three styles of magnetite mineralization, with averages ranging from 0.46 – 0.62 wt

Table 1. Microprobe analysis of magnetite and ilmenite from intercumulus and semi-massive mineralization

Magnetite analysis with FeO and Fe_2O_3 calculated from stoichiometry (after Droop 1987)

Sample number	JHC-13-034							JHC-13-034								JHC-13-033				
mineralization style	intercumulus							intercumulus								semi-massive				
mineral habit	coarse magnetite						**Average**	magnetite lamellae in ilmenite							**Average**	coarse magnetite				**Average**
TiO_2	0.29	0.66	0.09	0.53	0.06	0.22	**0.31**	15.93	15.63	16.65	16.37	15.94	15.62	14.51	**15.81**	6.26	3.31	7.51	4.14	**5.30**
SiO_2	0.00	0.00	0.00	0.02	0.00	0.00	**0.00**	0.00	0.00	0.00	0.00	0.00	0.00	0.00	**0.00**	0.00	0.00	0.00	0.00	**0.00**
Al_2O_3	0.30	0.31	0.34	0.26	0.36	0.31	**0.31**	0.20	0.13	0.17	0.15	0.15	0.18	0.15	**0.16**	1.03	1.14	0.69	2.06	**1.23**
Cr_2O_3	0.05	0.05	0.05	0.03	0.05	0.04	**0.04**	0.04	0.04	0.02	0.05	0.05	0.05	0.03	**0.04**	0.01	0.01	0.02	0.00	**0.01**
V_2O_5	0.40	0.37	0.39	0.42	0.62	0.57	**0.46**	0.63	0.66	0.53	0.62	0.62	0.60	0.65	**0.62**	0.51	0.61	0.52	0.66	**0.57**
FeO^{tot}	91.84	92.73	92.95	91.70	92.65	93.84	**92.62**	75.54	76.24	74.90	75.97	76.90	76.85	78.09	**76.36**	86.04	88.63	84.60	87.71	**86.75**
FeO-calc	31.00	31.81	31.16	31.31	31.13	31.59	**31.33**	43.81	43.67	44.30	44.37	44.42	43.87	43.07	**43.93**	34.91	32.94	35.60	33.35	**34.20**
Fe_2O_3-calc	67.61	67.70	68.66	67.11	68.37	69.18	**68.11**	35.27	36.20	34.01	35.11	36.10	36.65	38.92	**36.04**	56.82	61.88	54.46	60.41	**58.39**
MnO	0.04	0.00	0.02	0.00	0.01	0.02	**0.01**	0.07	0.08	0.10	0.09	0.10	0.08	0.07	**0.08**	0.29	0.15	0.38	0.20	**0.26**
NiO	0.00	0.02	0.00	0.02	0.00	0.06	**0.02**	0.00	0.03	0.03	0.01	0.00	0.02	0.00	**0.01**	0.00	0.03	0.00	0.00	**0.01**
ZnO	0.02	0.00	0.00	0.00	0.00	0.06	**0.01**	0.00	0.01	0.00	0.01	0.00	0.00	0.00	**0.00**	0.00	0.00	0.00	0.00	**0.00**
MgO	0.15	0.13	0.18	0.16	0.16	0.18	**0.16**	0.62	0.57	0.67	0.66	0.45	0.56	0.49	**0.57**	1.44	0.99	1.55	1.59	**1.39**
CaO	0.02	0.00	0.00	0.00	0.02	0.00	**0.01**	0.00	0.00	0.00	0.01	0.01	0.05	0.02	**0.01**	0.01	0.00	0.00	0.01	**0.01**
Total	99.87	101.06	100.91	99.86	100.78	102.23	**100.78**	96.57	97.03	96.48	97.45	97.85	97.67	97.91	**97.28**	101.28	101.06	100.71	102.41	**101.37**

Ilmenite analysis with FeO and Fe_2O_3 calculated from stoichiometry (after Droop 1987)

Sample number	JHC-13-034												JHC-13-033				
mineralization style	intercumulus												semi-massive				
mineral habit	Coarse ilmenite with magnetite lamellae											**Average**	coarse Ilmenite				**Average**
TiO_2	43.12	44.48	47.60	47.96	48.72	48.06	50.38	48.60	46.03	48.00	49.15	**47.46**	51.42	53.61	51.38	53.85	**52.56**
SiO_2	0.00	0.00	0.00	0.00	0.00	0.00	0.00	0.00	0.01	0.03	0.00	**0.00**	0.00	0.00	0.00	0.00	**0.00**
Al_2O_3	0.03	0.04	0.02	0.05	0.03	0.04	0.06	0.03	0.04	0.08	0.06	**0.04**	0.08	0.07	0.09	0.07	**0.07**
Cr_2O_3	0.02	0.02	0.00	0.03	0.00	0.00	0.00	0.00	0.05	0.00	0.00	**0.01**	0.00	0.00	0.00	0.03	**0.01**
V_2O_5	0.24	0.24	0.21	0.27	0.22	0.26	0.20	0.20	0.23	0.18	0.07	**0.21**	0.03	0.08	0.12	0.04	**0.07**
FeO^{tot}	52.89	52.99	50.28	49.50	48.64	48.48	47.34	48.10	51.47	48.92	47.78	**49.67**	42.59	40.71	41.80	39.39	**41.12**
FeO-calc	34.53	35.52	38.68	38.17	41.00	38.29	41.38	38.66	37.08	38.48	39.22	**38.27**	36.04	36.97	35.65	36.84	**36.38**
Fe_2O_3-calc	20.41	19.41	12.90	12.59	8.49	11.32	6.63	10.49	15.99	11.60	9.52	**12.67**	7.28	4.16	6.84	2.83	**5.28**
MnO	0.37	0.40	0.46	0.42	0.56	0.45	0.52	0.47	0.49	0.42	0.45	**0.46**	0.64	0.85	0.75	0.99	**0.81**
NiO	0.00	0.00	0.00	0.01	0.00	0.00	0.05	0.00	0.02	0.03	0.03	**0.01**	0.02	0.01	0.02	0.02	**0.02**
ZnO	0.02	0.00	0.00	0.01	0.05	0.05	0.02	0.03	0.05	0.01	0.03	**0.03**	0.00	0.00	0.02	0.01	**0.01**
MgO	2.16	2.28	2.05	2.53	1.22	2.48	1.84	2.54	2.11	2.38	2.50	**2.19**	5.34	5.81	5.47	5.90	**5.63**
CaO	0.00	0.01	0.00	0.00	0.02	0.00	0.04	0.00	0.00	0.02	0.01	**0.01**	0.00	0.01	0.00	0.02	**0.01**
Total	100.91	102.39	101.90	102.05	100.30	100.95	101.11	101.04	102.09	101.23	101.03	**101.36**	100.86	101.55	100.33	100.61	**100.83**

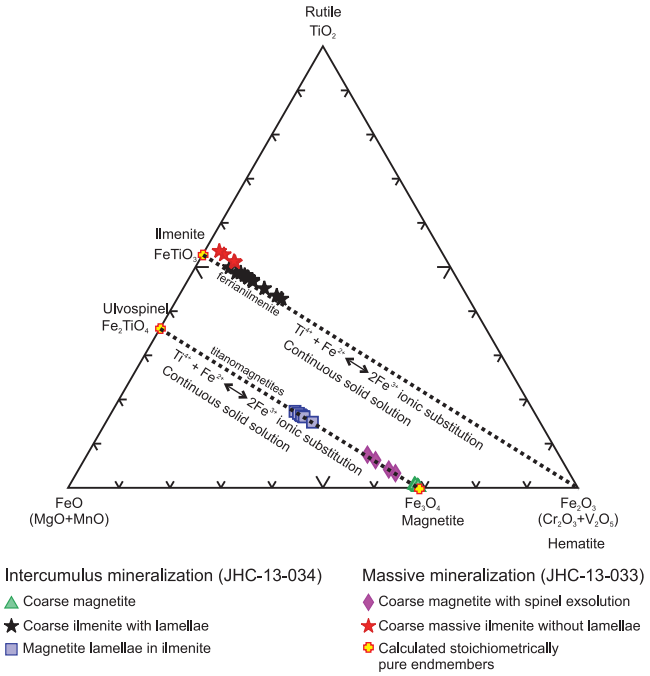

Figure 2. *Composition of oxide minerals in the system TiO_2–FeO–Fe_2O_3 (subordinate oxides added where appropriate).* See *text for discussion.*

%. The titanomagnetite lamellae in the disseminated intercumulus mineralization and the coarse-grained magnetite in the semi-massive to massive mineralization have the highest concentrations (Table 1). Coarse magnetite from the semi-massive to massive style of mineralization also contains increased proportions of MgO and MnO (Table 1), representing partial substitution for Fe^{2+} compared to the disseminated style of mineralization, and increased Al_2O_3, representing partial substitution for Fe^{3+} resulting in spinel exsolution.

Ilmenite compositions also vary in FeO^T and TiO_2 compositions, with the coarse-grained massive ilmenite in the semi-massive to massive mineralization having higher TiO_2 and lower FeO^T than the ilmenite with titanomagenite lamellae in the disseminated intercumulate mineralization (Table 1). There is also substantially more MgO and MnO in the coarse-grained semi-massive to massive variety of ilmenite mineraliziation (Table 1). In terms of V_2O_5 contents, the coarse-grained ilmenite displaying the titanomagnetite lamellae in the disseminated intercumulate mineralization contains significantly more V than the ilmenite in the semi-massive style of mineralization (Table 1). However, electron microprobe work shows that some of the ilmenite contains very fine-scale magnetite lamallae (*e.g.*, lamellae within lamellae), and these might be the host for the V.

LITHOGEOCHEMISTRY

INTRODUCTION AND LIMITATIONS

A representative suite of all plutonic rock types from the Keating Hill prospect were analyzed for major, trace and rare-earth elements at the GSNL geochemical laboratory. Major elements were analyzed using ICP-OES-fusion methods; most of the trace elements were analyzed by ICP-MS-fusion methods, and the remainder of the trace elements being analyzed via ICP-OES-4-acid methods. The full geochemical dataset and analytical methods used for each element will be released in a subsequent open-file report. All samples presented in this report were collected from diamond-drill core from five drillholes on the Keating Hill prospect (total of 61 samples).

Before attempting to present and interpret lithogeochemical data from this study, it is important to explain some of the limitations of the data. The rocks discussed within this report have cumulate textures, and as such the determined chemical compositions do not represent any parental magma liquid composition. The original magma composition has been modified by processes such as fractional crystallization and mineral accumulation, and it is difficult to assess results in terms of magmatic evolution processes. The results are, however, useful for an interpretative approach examining cumulate and accessory mineral contents and compositional variation between rock types. As all rocks also contain variable amounts of oxide and sulphide minerals, major and trace elements such as TiO_2, FeO, Fe_2O_3, Ni, and Cu are strongly influenced by the proportion of mineralization.

MAJOR AND MINOR ELEMENTS

Most samples from the Keating Hill prospect have low loss-on-ignition values (<0.8%), a result consistent with the generally fresh nature of the rocks. The data show large ranges in major-element concentrations; illustrated through the use of Harker diagrams (Figure 3) and drillhole chemostratigraphy (Figure 4). Concentrations of $Fe_2O_3^T$, TiO_2, and V_2O_5 all show strong negative correlations with SiO_2, indicative of Fe–Ti oxide control (Figure 3A–C). This is also observed on the chemostratigraphic profile illustrated in Figure 4 in which the semi-massive oxide units plot with significantly increased proportions of Fe_2O_3, TiO_2, and V_2O_5. A positive correlation exists both between Al_2O_3 and CaO when plotted against SiO_2; with the more leucocratic samples having the higher concentrations of Al_2O_3 and CaO indicative of cumulate plagioclase control (Figure 3D, E).

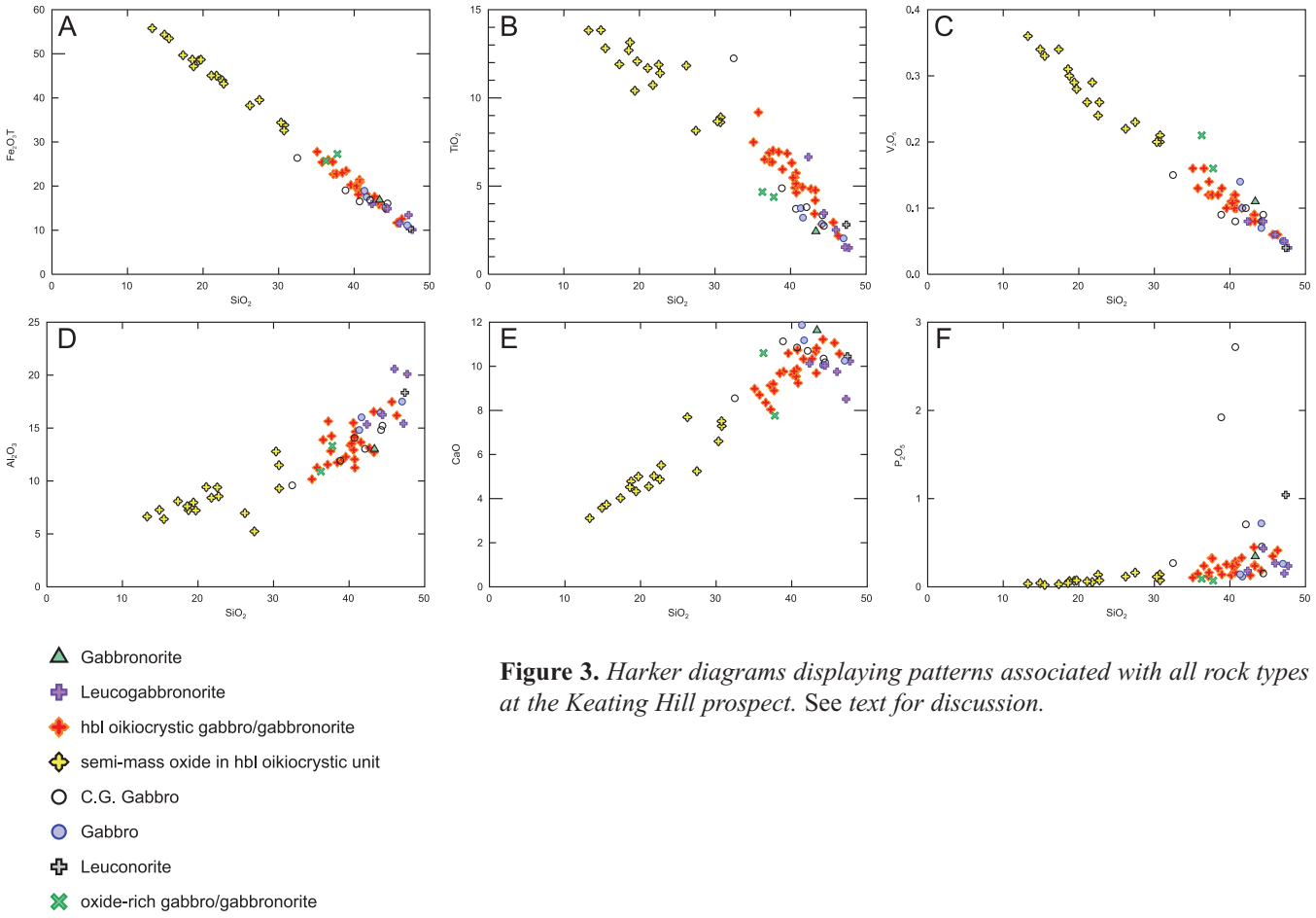

Figure 3. *Harker diagrams displaying patterns associated with all rock types at the Keating Hill prospect.* See *text for discussion.*

The P_2O_5 against SiO_2 shows a set of samples with relatively high P_2O_5 concentrations indicative of cumulus apatite as observed petrographically, whereas the bulk of the samples have lower P_2O_5 values (<1 wt %) displaying a positive trend against SiO_2, indicative of control by cumulus apatite as well as trapped liquid (Figure 3F).

Plots of $Fe_2O_3^T$ *vs* TiO_2 and $Fe_2O_3^T$ *vs* V_2O_5 show positive correlations indicative of magnetite–ilmenite control (Figure 5A, B). A similar pattern is observed in the plot of TiO_2 *vs* V_2O_5 (Figure 5C). It is noted that the samples of the oxide-rich gabbro/gabbronorite (lacking the hornblende oikocrysts) plot with a slightly higher relative concentration of V_2O_5 and a slightly lower relative concentration of TiO_2 compared to the trends defined by most rocks (Figure 5A–C); perhaps indicative of a primarily magnetite control on vanadium concentrations. A positive correlation between Ni and Cu (Figure 5D) suggests that these elements are controlled by base-metal sulphides, as expected based on petrographic observations.

TRACE ELEMENTS

Concentrations of total rare-earth elements (REEs) show positive correlations with P_2O_5 contents in most rocks (Figure 6A); indicative of the control that minerals such as apatite exert on abundance of REEs. In contrast, concentrations of other trace elements, most notably the high-field-strength elements (HFSE) such as Hf, Zr, Nb and Ta do not display a positive correlation with P_2O_5; suggesting that there are other controls on their distribution (*e.g.*, Hf *vs* P_2O_5 displayed in Figure 6B).

Rare-earth-element concentrations in rock types range in abundance from approximately 2 to 300 times chondrite, with the coarse-grained gabbroic rocks having the highest concentrations and the semi-massive oxide mineralization having the lowest concentrations (Figure 7). The overall high concentrations of REE are interpreted to be linked to variable quantities of intercumulus trapped liquids in the cumulate rocks; as observed through the SEM–MLA work

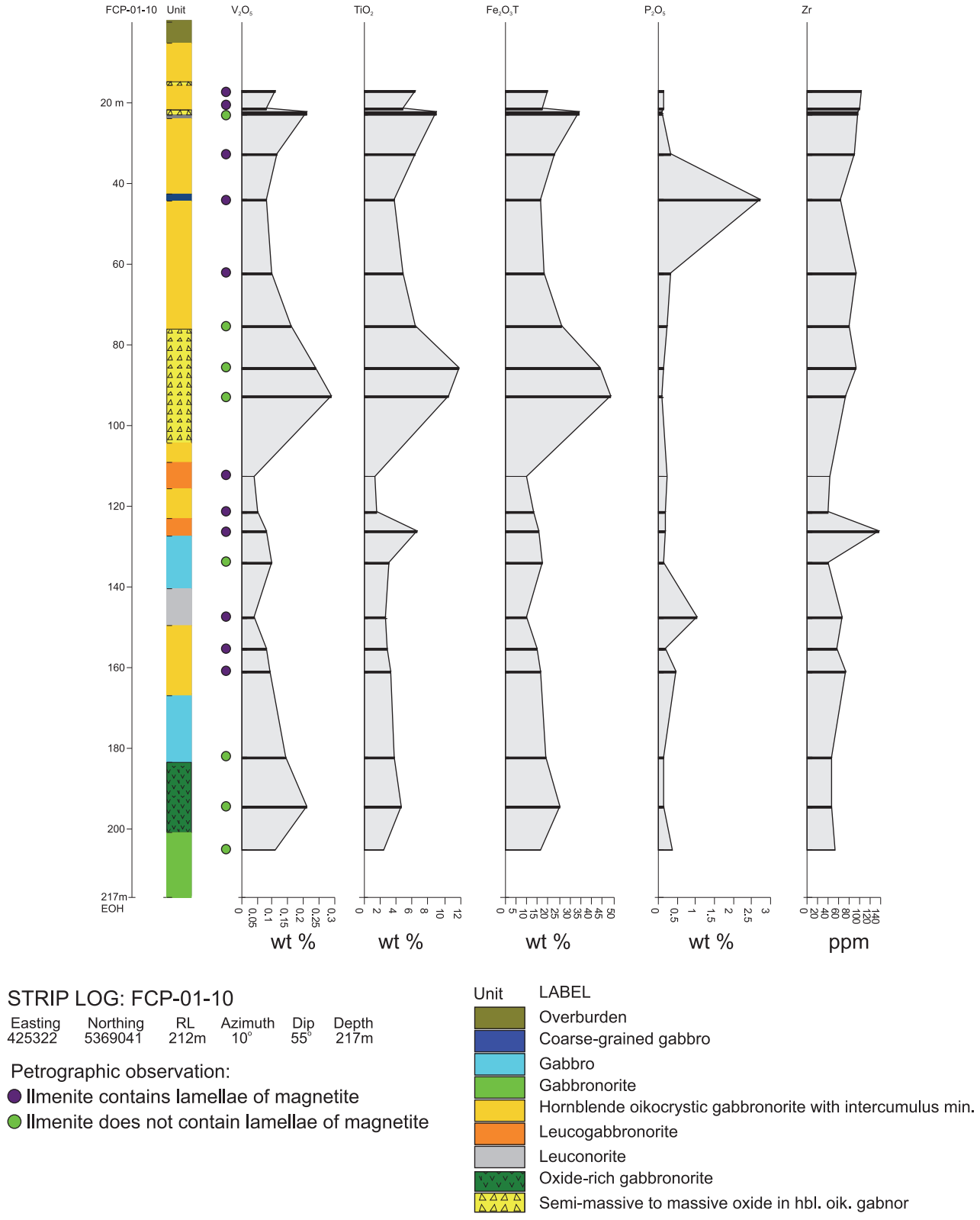

Figure 4. *Downhole striplog of DDH FCP-01-10 illustrating the correlation of the higher grade $Fe_2O_3^T$, TiO_2, and V_2O_5 concentrations with the semi-massive oxide hornblende oikocrystic unit observed during diamond-drill hole logging. Note also that the higher grade semi-massive oxides do not contain titanomagnetite lamellae in the ilmenite (green circles) whereas the disseminated oxides do (purple circles).*

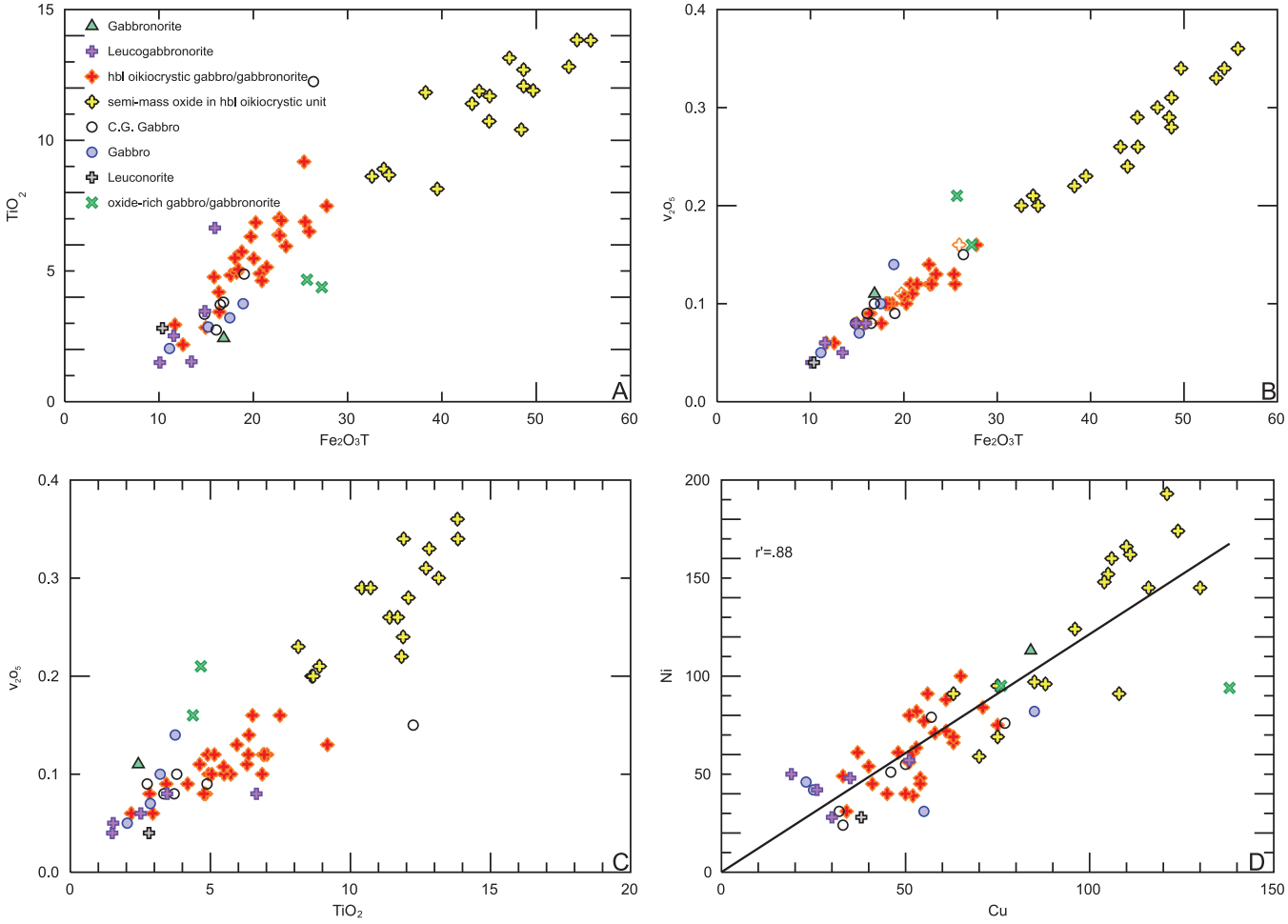

Figure 5. *Bimodal major- and trace-element plots illustrating oxide and sulphide controls on Fe, Ti, V, Ni, and Cu.* See *text for details.*

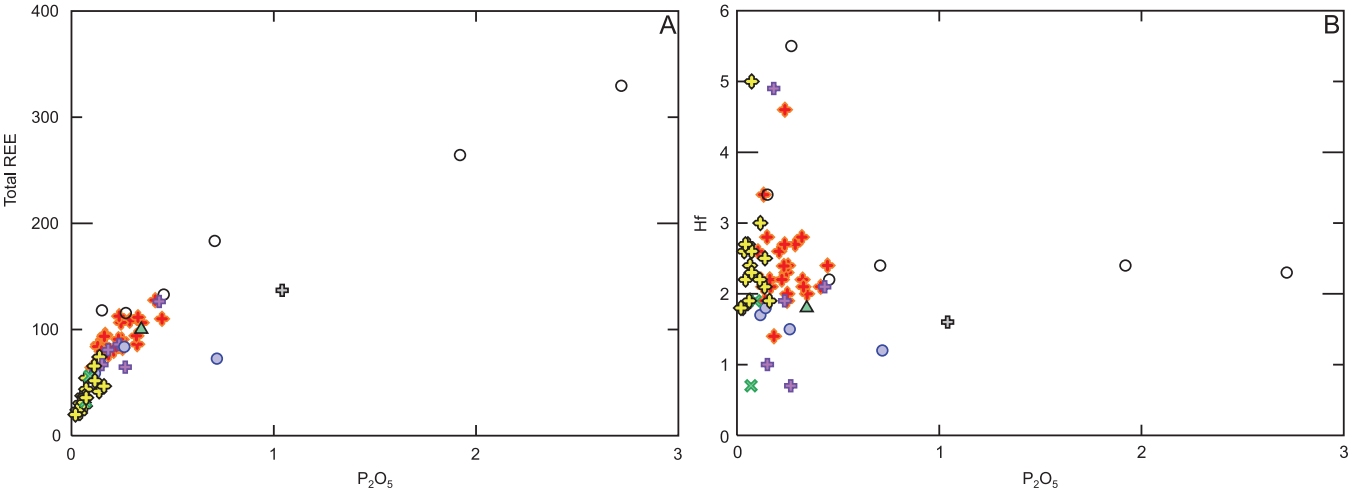

Figure 6. A) *Total REE* versus P_2O_5 *plot illustrating a positive correlation; indicative of the dominant control that cumulate and intercumulate minerals, such as apatite, exert on the abundance of REEs; and* B) *Plot of* P_2O_5 versus *Hf as an illustration that the HFSE are not controlled solely by the presence of apatite or other intercumulate phosphate minerals.*

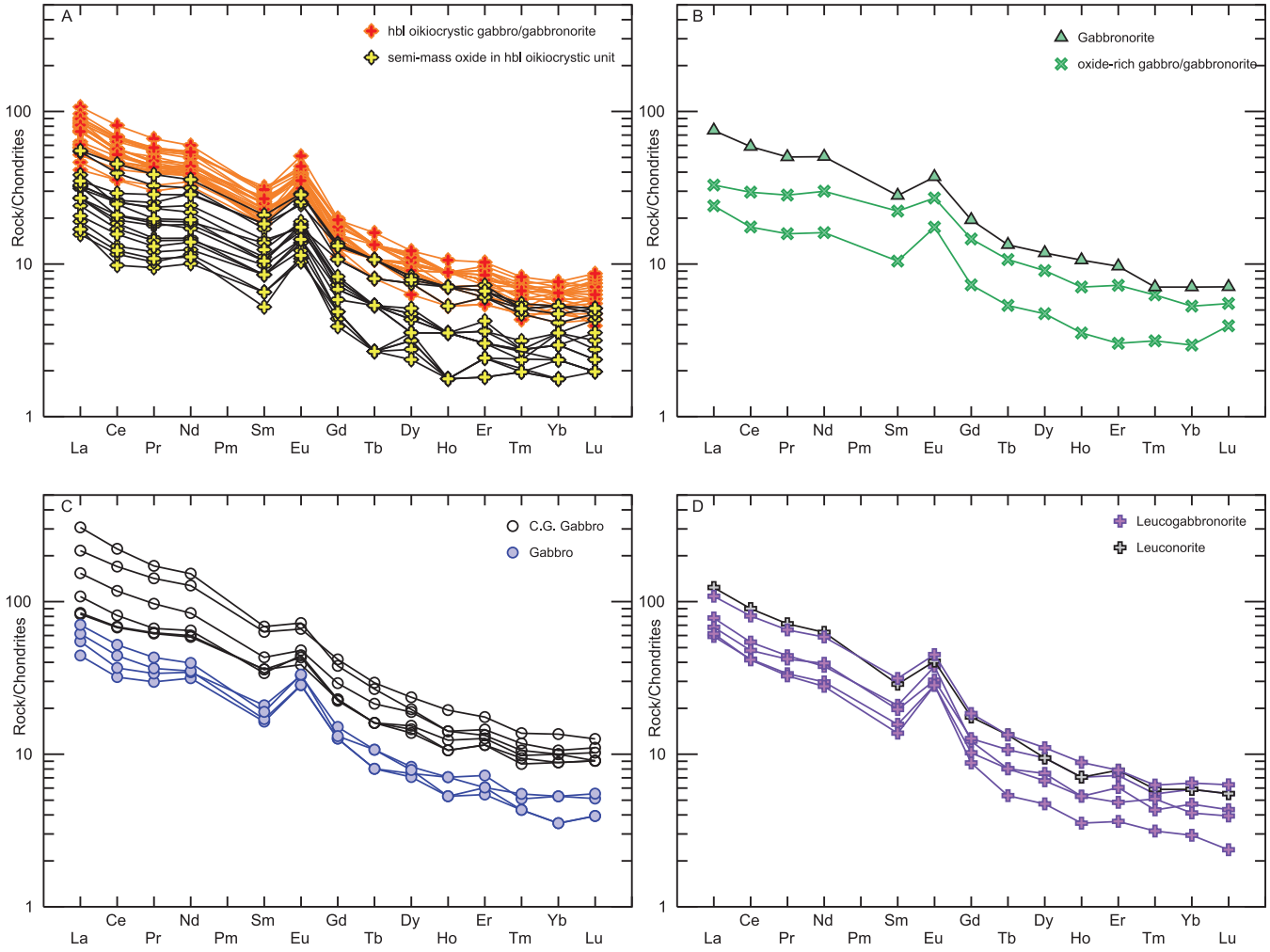

Figure 7. A–D) *Chondrite-normalized REE patterns for all rock types at the Keating Hill prospect. Note the similar patterns for all rock types including enrichment in the LREE compared to the MREE and HREE, as well as positive Eu anomalies related to the presence of cumulate plagioclase.* See *text for further discussion. Normalizing values are from Sun and McDonough (1989).*

described above. The extraordinarily high concentrations in the coarse-grained rocks are related to the presence of cumulus apatite. Rare-earth-element patterns from all rock types display similar normalized patterns with the light REE being enriched relative to the middle and heavy REE (Figure 7A–D). All rocks display positive europium anomalies attributed to ubiquitous cumulate plagioclase.

The concentrations of REE and other trace elements are displayed on primitive mantle-normalized extended trace-element plots in Figure 8A–D. Excluding the low-field-strength elements (LFSE) Rb and Ba, most trace-element concentrations range from approximately 0.5 to 100 times primitive mantle (Figure 8A–D). The primitive mantle-normalized spider diagrams illustrate a number of common features between most rock types, with the semi-massive to massive mineralization showing variations in the patterns for some elements. All rock types, excluding the semi-massive to massive mineralized rocks, consistently display negative anomalies with respect to the high-field-strength elements (Th, Nb, Zr, Hf) and positive anomalies with respect to Ba, Sr and sporadically P (Figure 8A–D). In contrast, the semi-massive to massive mineralized hornblende oikocrystic gabbronorite commonly displays lower relative concentrations of most trace elements compared to the other associated weakly mineralized rocks, but they display positive primitive mantle-normalized anomalies for Nb, Ta, Zr, and Hf (Figure 8A). Of interest, as with most of the trace elements, the semi-massive mineralized gabbronorite contains lower relative concentrations of P than the other rock types. This would suggest that the HFSE (Nb, Ta, Zr, and Hf) are controlled by some mineral than apatite. The most likely explanation is that they are hosted within the oxide mineralization (*e.g.*, *see* Nielsen and Beard, 2000; Bai *et al*., 2012).

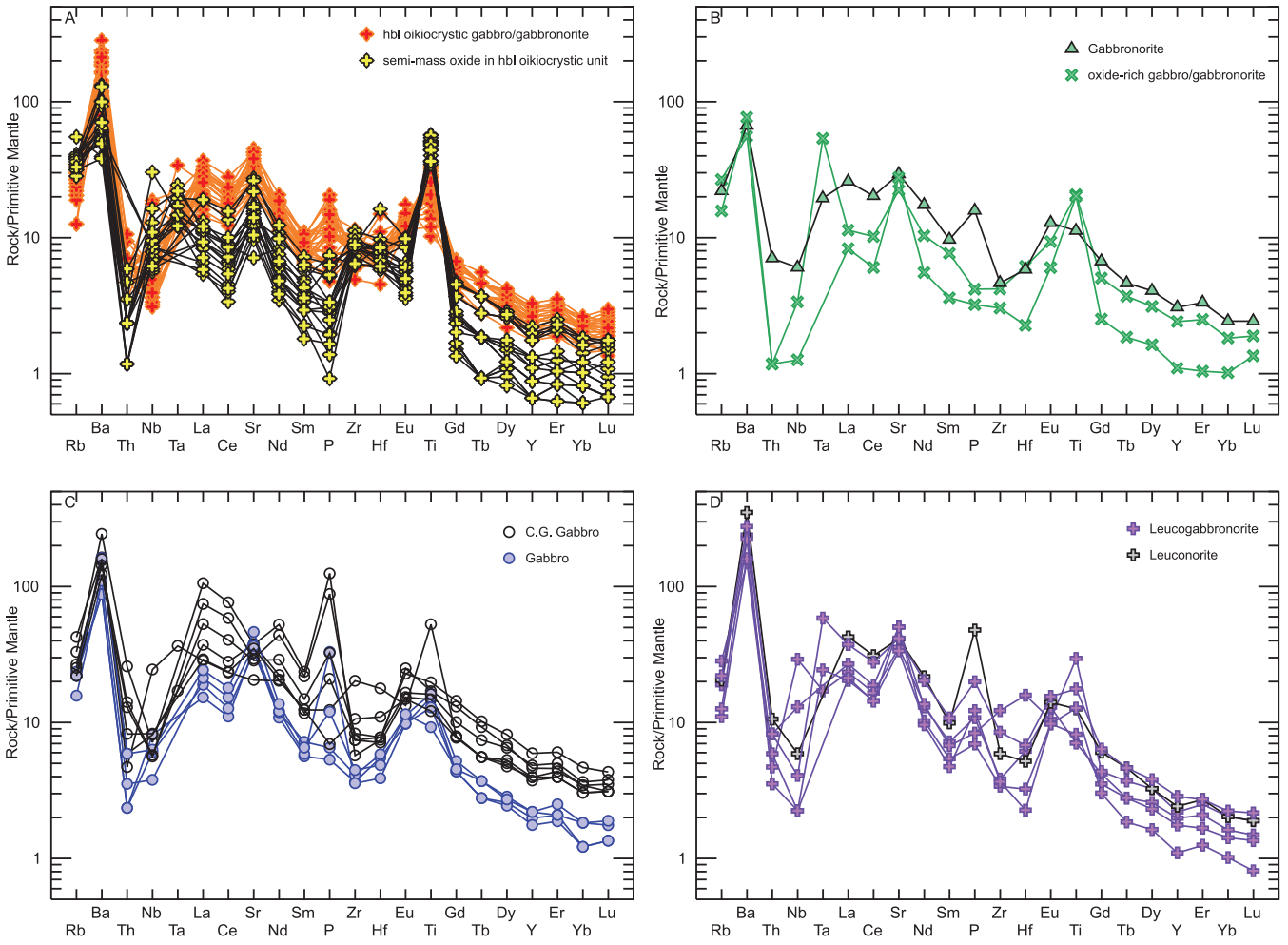

Figure 8. A–D) *Extended trace-element-normalized plots for all rock types from the Keating Hill prospect. Notice that all rock types with the exception of the semi-massive to massive mineralization display negative anomalies for the HFSE's including Th, Nb, Zr and Hf. In contrast, the semi-massive to massive mineralization displays positive primitive-mantle-normalized anomalies for the HFSE. Normalizing values are from Sun and McDonough (1989).*

Accepting the presumption that the semi-massive to massive mineralization is hosted by the same hornblende oikocrystic gabbronorite that contains the intercumulus oxide mineralization; then, these relationships are easily illustrated in Figure 9A and B. Figure 9A compares the semi-massive mineralization patterns with that of the average pattern derived from all of the hornblende oikocrystic gabbronorite with inter-cumulate mineralization, whereas Figure 9B normalizes the compositions of the semi-massive to massive invasive mineralization samples to the average composition of the hornblende oikocrystic gabbronorite.

SUMMARY AND DISCUSSION

The Silurian magmatic oxide mineralization at the Keating Hill prospect represents a newly recognized style of mineralization for Newfoundland. It is emphasized that, although numerous examples of magmatic sulphide occurrences have been described from mafic Silurian–Devonian intrusions in central and western Newfoundland (*e.g.*, Kerr, 1999; Hinchey, 2013), the Keating Hill prospect is currently the only known example of significant oxide mineralization.

STYLES OF MINERALIZATION

There are at least two styles of oxide mineralization, both of which are hosted by a hornblende oikocrystic gabbronorite that is interpreted to represent a single intrusive rock unit. There is an early magmatic oxide mineralization style developed by fractional crystallization processes involving the gravitational settling and sorting of intercumulus oxide liquids, and a later style in which immiscible oxide liquid was injected into the cumulate pile forming massive oxide layers or lenses that appear to be invasive.

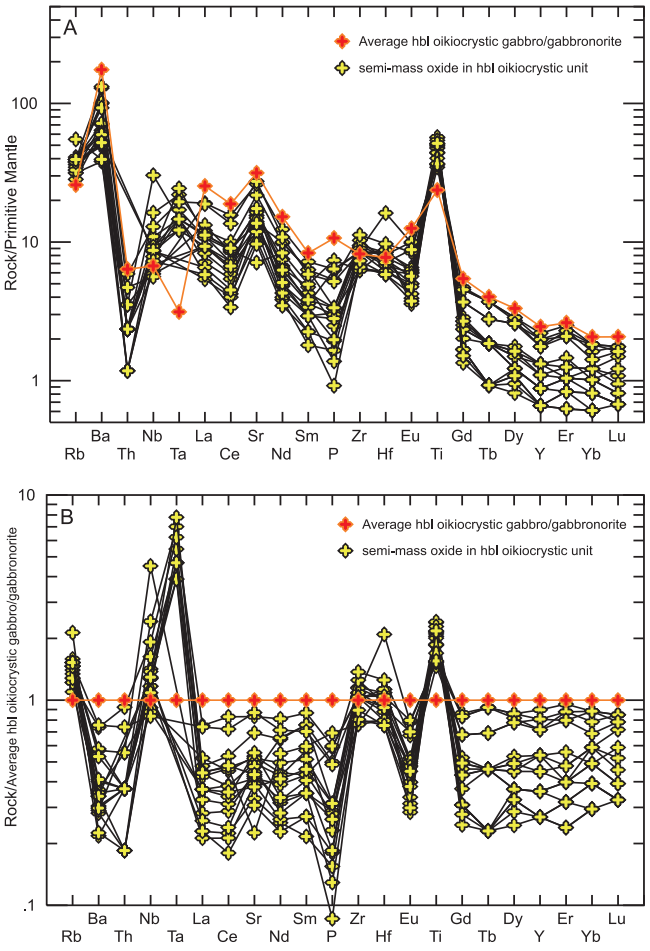

Figure 9. A) *Extended primitive-mantle-normalized trace-element plot comparing the patterns from semi-massive to massive oxide mineralized rocks with that of the average for the hornblende oikocrystic gabbronorite with intercumulus mineralization; and* B) *Extended trace-element plot with the semi-massive to massive mineralized rocks normalized to the average composition of the hornblende oikocrystic gabbronorite with intercumulus oxide mineralization.*

The first style of mineralization is represented by intercumulus oxide mineralization, which appears to have a magmatic origin. This style of mineralization is similar to that envisioned for primary magmatic sulphide deposits that share many textural relationships with the oxide mineralization discussed herein.

The second, perhaps more economically important, style of mineralization occurs as semi-massive to massive oxides. This style of mineralization has abrupt upper and lower contacts with the host hornblende oikocrystic gabbronorite. The oxide mineralization fills spaces between, or more commonly totally encloses, silicate minerals dominated by plagioclase and pyroxene. The massive oxide mineralization also locally contains inclusions of more leucocratic gabbro with much less oxide mineralization. Initial field observations of hand specimens suggested that the plagioclase crystals were cumulate, based on their elongated and lath-type shapes; however, subsequent petrographic investigations displayed distinct mineralogical textures that suggested silicate-oxide disequilibrium conditions. This textural evidence supports the hypothesis that the oxide minerals crystallized from an oxide-rich melt or liquid that was injected into a plagioclase-rich crystal mush. Hence, the semi-massive to massive oxide mineralization did not form through simple fractional crystallization processes as envisaged for the intercumulus mineralization.

It should be noted that although the semi-massive to massive mineralization is interpreted to have formed after the silicate minerals had formed into a crystal mush, the mineralization is still broadly magmatic. The large density contrast between such an oxide-rich melt or liquid and the host silicate rocks would likely physically limit the potential migration distances that any oxide melt could travel; especially given the partial crystallization of the host hornblende oikocrystic gabbronorite cumulate rocks and the relatively low volatile contents of the oxide mineralization. It is therefore postulated that the oxide liquid that was injected into the silicate crystal pile was most likely derived from the same magma chamber that produced the host rocks. Oxide mineral chemistry variations between the styles of mineralization (*see* above), and the higher concentrations of high-field-strength elements in massive mineralization, may indicate derivation from different magma pulses or batches.

It is not clear why this magmatic system developed into oxide-rich mineralization. The increased proportions of oxide minerals are most likely related to variations in the Fe_2O_3/FeO ratio of parental liquids, which in turn are related to temperature, oxygen fugacity, and the water content of the magma. The presence of hornblende and biotite suggests that the intrusions were hydrous and this was likely an important factor, potentially leading to oxide and silicate liquid immiscibility. The presence of rounded magmatic sulphide blebs in equilibrium with the oxide minerals constrains the upper limit for oxygen fugacity.

Well-studied examples of similar styles of mineralization occur in intrusions related to the *ca.* 260 Ma Emeishan Large Igneous Province in southwest China (*e.g.*, *see* Zhou *et al*., 2005; Pang *et al*., 2008; Bai *et al*., 2012; Zhou *et al*., 2013; Song *et al*., 2013; Howarth *et al*., 2013). Many of these studies also describe contrasting models and styles of oxide mineralization that resemble those described in this report, supporting the notion that two or more generations and styles of oxide mineralization may be feasible within one magmatic system.

CONCLUSIONS AND IMPLICATIONS

Results from this study deliver the following conclusions and implications:

1) There are two different styles of oxide mineralization. Although these are distinct in oxide mineral chemistry and textures, they are both interpreted to have formed in the same magma chamber through magmatic processes.
2) Disseminated intercumulus oxide mineralization is easily explained through processes of fractional crystallization and evolution of intercumulate liquids, but the formation of the invasive style of semi-massive to massive oxide mineralization is more complicated. The working model of formation involves development of an immiscible hydrous Fe-Ti rich liquid, which was subsequently injected into a crystal mush to produce discrete semi-massive to massive mineralized zones.
3) Results imply that other Silurian mafic intrusions in central and western Newfoundland may have potential to host similar oxide-rich mineralization as that observed at the Keating Hill prospect, although examples have yet to be documented.
4) Observations of contrasting oxide compositions and textures between the two mineralization styles may be important for evaluation of metallurgical characteristics of this mineralization.

ACKNOWLEDGMENTS

Paul Neal and Alexander Calon provided capable assistance while conducting field work and Gerry Hickey helped with logistics and safety. Stephen Piercey is thanked for assistance with the MLA–SEM work and image processing at Memorial University of Newfoundland, and Peter Jones is thanked for the thorough and well-documented electron microprobe data. Hamish Sandeman is thanked for numerous discussions on the implications of the geochemical data discussed in this report. Triple Nine Resources personnel are thanked for allowing access to the property and for a field visit to the property. This manuscript has benefitted from reviews by Andy Kerr and Charles Gower.

REFERENCES

Bai, Z.J., Hong, Z., Naldrett, A.J., Zhu, W.G. and Xu, G.W.
2012: Whole-rock and mineral composition constraints on the genesis of the giant Hongge Fe-Ti-V oxide deposit in the Emeishan Large Igneous Province, Southwest China. Economic Geology, Volume 107, pages 507-524.

Barnes, F.Q., Riley, G.C. and Smith, C.H.
1957: Geological Survey of Canada, Preliminary Map 2-1957, Stephenville, Newfoundland; 1 sheet, doi:10.4095/124131

Carew, W.
1979: A layered appinitic intrusion in southwest Newfoundland: a field, petrographical and geochemical investigation. Unpublished B.Sc. thesis, Memorial University of Newfoundland, St. John's, 53 pages.

Currie, K.L. and van Berkel, J.T.
1989: Geochemistry of post-tectonic mafic intrusions in the Central Gneiss Terrane of southwestern Newfoundland. Atlantic Geology, Volume 25, pages 181-190.

1992a: Geology, southern Long Range Mountains, Newfoundland, Geological Survey of Canada, Map 1815A, scale 1:100 000.

1992b: Notes to accompany a geological map of the southern Long Range, southwestern Newfoundland, Geological Survey of Canada, Paper 91-10, 10 pages.

Droop, G.T.R.
1987: A general equation for estimating Fe3+ concentrations in ferromagnesian silicates and oxides from microprobe analysis, using stoichiometric criteria. Mineralogical Magazine, Volume 51, pages 431-435.

Dunning, G.R., O'Brien, S.J., Colman-Sadd, S.P., Blackwood, R.F., Dickson, W.L., O'Neill, P.P. and Krogh, T.E.
1990: Silurian orogeny in the Newfoundland Appalachians. Journal of Geology, Volume 98, pages 895-913.

French, V.A. and Mugford, C.
2010: First and third year assessment report on geological, geochemical, geophysical, trenching and diamond drilling exploration for licenses 17369M and 17894M on claims in the Southwest Brook area, southwestern Newfoundland, 3 reports [NFLD/3237].

Hinchey, J.G.
2013: The geology and genesis of the Silurian Portage Ni–Cu and Ordovician Range Cu–Co showings, southwestern Newfoundland (NTS map area 12A/05): Preliminary results. *In* Current Research. Newfoundland and Labrador Department of Natural Resources, Geological Survey, Report 13-1, pages 99-116.

Howarth, G.H., Prevec, S.A. and Zhou, M.-F.
2013: Timing of Ti-magnetite crystallization and silicate disequilibrium in the Panzhihua mafic layered intrusion: Implications for ore-forming processes. Lithos, Volume 170-171, pages 73-89.

Kerr, A.
1999: The Powderhorn Lake Ni–Cu showings and the potential for magmatic sulphide mineralization in cen-

tral Newfoundland. *In* Current Research. Newfoundland and Labrador Department of Mines and Energy, Geological Survey, Report 99-1, pages 205-214.

Lissenberg, C.J., van Staal, C.R., Bédard, J.H. and Zagorevski, A.
2005: Geochemical constraints on the origin of the Annieopsquotch ophiolite. Geological Society of America Bulletin, Volume 117, pages 1413-1426.

Lissenberg, C.J., McNicoll, V.J. and van Staal, C.R.
2006: The origin of mafic-ultramafic bodies within the northern Dashwoods Subzone, Newfoundland Appalachians. Atlantic Geology, Volume 42, pages 1-12.

Nielsen, R.l. and Beard, J.S.
2000: Magnetite-melt HFSE partitioning. Chemical Geology, Volume 164, pages 21-34.

Pang, K.-N., Zhou, M.-F., Lindsley, D., Zhao, D. and Malpas, J.
2008: Origin of Fe-Ti oxide ores in mafic intrusions: Evidence from the Panzhihua intrusion SW China. Journal of Petrology, Volume 49, pages 295-313.

Pehrsson, S.J., Brem, A.G. and van Staal, C.R.
2013: Geology, Main Gut, Newfoundland and Labrador. Geological Survey of Canada, Open File 1666, scale 1:50 000, doi. 10.4095/292182

Riley, G.C.
1957: Red Indian Lake, west half, Newfoundland. Geological Survey of Canada, Preliminary Map 8-1957, 1:253 440 scale.

Sun, S.S. and McDonough, W.F.
1989: Chemical and isotopic systematics of ocean basalts: Implications for mantle composition and processes. Geological Society, Special Publication 42, pages 313-345.

Song, X.-Y., Qi, H.-W., Hu, R.-Z., Chen, L.-M. and Yu, S.-Y.
2013: Formation of thick stratiform Fe-Ti oxide layers in layered intrusion and frequent replenishment of fractionated mafic magma: Evidence from the Panzhihua intrusion, SW China. Geochemistry Geophysics Geosystems, Volume 14, pages 712-732.

Thomson, R.
1941: Preliminary report on C.H. McFairdge – J. Keating Magnetic Prospect, east of Stephenville Crossing, Newfoundland. Geological Survey of Canada, 3 pages [12A/5/13].

van Berkel, J.T.
1987: Geology of the Dashwoods Pond, St. Fintan's and Main Gut map areas, southwest Newfoundland. *In* Current Research, Part A. Geological Survey of Canada, Paper 87-1A, pages 399-408.

van Staal, C.R., Lissenberg, C.J., Pehrsson, S., Zagorevski, A., Valverde-Vaquero, P., Herd, R.K., McNicoll, V.J. and Whalen, J.
2005: Geology, Puddle Pond, Newfoundland and Labrador. Geological Survey of Canada, Open File 1664, scale 1:50 000.

van Staal, C.R., Whalen, J.B., McNicoll, V.J., Pehrsson, S., Lissenberg, C.J., Zagorevski, A., van Breemen, O. and Jenner, G.A.
2007: The Notre Dame arc and the Taconic orogeny in Newfoundland. *In* 4-D Framework of Continental Crust. *Edited by* R.D., Jr., Hatcher, M.P. Carlson, J.H. McBride and J.R. Martínez Catalan. Geological Survey of America, Memoir 200, pages 511-552.

Whalen, J.B., McNicoll, V.J., van Staal, C.R., Lissenberg, C.J., Longstaffe, F.J., Jenner, G.A. and van Breeman, O.
2006: Spatial, temporal and geochemical characteristics of Silurian collision-zone magmatism, Newfoundland Appalachians: An example of a rapidly evolving magmatic system related to slab break-off. Lithos, Volume 89, pages 377-404.

Williams, H.
1995: Geology of the Appalachian-Caledonian Orogen in Canada and Greenland. Geological Survey of Canada, Geology of Canada: Temporal and Spatial Divisions; Chapter 2, pages 21-44.

Zagorevski, A., van Staal, C.R. and McNicoll, V.J.
2007: Distinct Taconic, Salinic, and Acadian deformation along the Iapetus suture zone, Newfoundland Appalachians. Canadian Journal of Earth Sciences, Volume 44, pages 1567-1585.

Zhou, M.-F., Robinson, P.T., Lesher, C.M., Keays, R.R., Zhang, C.-J. and Malpas, J.
2005: Geochemistry, petrogenesis and metallogenesis of the Panzhihua gabbroic layered intrusion and associated Fe-Ti-V oxide deposits, Sichuan Province, SW China. Journal of Petrology, Volume 46, pages 2253-2280.

Zhou, M.-F., Chen, W.T., Wang, C.Y., Prevec, S.A., Liu, P.P. and Howarth, G.H.
2013: Two stages of immiscible liquid separation in the formation of Panzhihua-type Fe-Ti-V oxide deposits, SW China. Geoscience Frontiers, Volume 4, pages 481-502.